



# Influence of pressure of nitrogen gas on structure and thermoelectric properties of acid-treated PEDOT:PSS films

May Thu Zar Myint<sup>1,2</sup> · Hirotaka Inoue<sup>1</sup> · Susumu Ichimura<sup>3</sup> · Takeshi Nishikawa<sup>1</sup> · Yuta Nishina<sup>1</sup> · Aung Ko Ko Kyaw<sup>4</sup> · Yasuhiko Hayashi<sup>1</sup>

Received: 13 April 2019 / Accepted: 19 June 2019 / Published online: 3 July 2019  
© Springer Science+Business Media, LLC, part of Springer Nature 2019

## Abstract

Poly(3,4-ethylenedioxythiophene):poly(styrenesulfonate) (PEDOT:PSS) is the most commonly investigated conductive polymer due to its unique thermoelectric properties. Several post treatments using various acids have been reported to improve the thermoelectric properties of PEDOT:PSS. In most articles, however, only the role of acids on the structure and thermoelectric properties of PEDOT:PSS were reported. In this article, we report the major role of the pressure of nitrogen gas (N<sub>2</sub>) on the structure and thermoelectric properties of PEDOT:PSS after treatment with various acids at optimized temperatures. After treatment with acids followed by N<sub>2</sub> gas-passing, electrical conductivity enhances significantly. Therefore, N<sub>2</sub> gas-passing after acid treatments results in higher thermoelectric properties than other traditional acid treatment methods. The enhancement in electrical conductivity is attributed to the removal of insulating PSS and the conformational change of the PEDOT chain. Furthermore, the pressure of N<sub>2</sub> is responsible for the additional conformation of PEDOT chain, favoring the linear orientation of the PEDOT structure and resulting in an improvement of the electrical conductivity.

## 1 Introduction

The major portion of today's energy supply originates from fossil fuels and, which induce pollution and environmental problems [1–3]. However, energy is wasted as heat from automobile engines, industries, motors and power systems during their operation every day. Energy harvesting devices enable the conversion of wasted heat to energy for various applications [4, 5]. Thermoelectric (TE) material which can convert heat to electrical energy and vice versa, could help to

address this issue by recycling the waste heat [6, 7]. The efficiency of the thermoelectric material is defined by dimensionless figure of merit,  $ZT = S^2\sigma T/\kappa$ , where  $S$  is the Seebeck coefficient,  $\sigma$  is the electrical conductivity,  $T$  is the absolute temperature and  $\kappa$  is the thermal conductivity [8–10].

Owing to the discovery and development of conductive polymers by Heeger, Macdiarmid and Shirakawa, it has been used in a wide range of electronic applications [11, 12]. Poly(3,4-ethylenedioxythiophene)(PEDOT): poly styrene sulfonate (PSS) has advantages over other conductive polymers due to its outstanding properties such as easy processing, high electrical conductivity, stability and flexibility [13, 14]. On the other hand, TE performance of PEDOT:PSS are still lower for its practical uses due to the excess insulating PSS in the PEDOT:PSS dispersion. Moreover, PSS molecules play an important role in PEDOT:PSS as counter ions as well as dispersion agent for PEDOT. Therefore, it is necessary to selectively remove the excess PSS to improve electrical conductivity of PEDOT:PSS [15, 16]. Previous works have employed the post-treatment of PEDOT:PSS films with various acids to improve the TE properties by controlling the doping level. Nevertheless, only the effect of acids or organic solvents on the structure and thermoelectric properties of the PEDOT:PSS are focused in their reports [10, 16–19]. In this article, we report the post-treatment of PEDOT:PSS films

✉ Aung Ko Ko Kyaw  
aung@sustech.edu.cn

✉ Yasuhiko Hayashi  
hayashi.yasuhiko@okayama-u.ac.jp

<sup>1</sup> Graduate School of Natural Science and Technology, Okayama University, Okayama 700-8530, Japan

<sup>2</sup> Faculty of Advanced Materials Engineering, University of Technology (Yatanarpon Cyber City), Pyin Oo Lwin District, Mandalay, Myanmar

<sup>3</sup> Nagoya Industries Promotion Corporation, 3-4-41 Rokuban, Atsuta, Nagoya 456-0058, Japan

<sup>4</sup> Department of Electrical and Electronic Engineering, Southern University of Science and Technology, Shenzhen 518055, People's Republic of China

with various acids followed by N<sub>2</sub> gas-passing. The influence of the pressure of N<sub>2</sub> gas on the structure and thermoelectric properties of PEDOT:PSS at various pressures are also discussed. The electrical conductivity significantly improved from less than 1 Scm<sup>-1</sup> to 1810 ± 200 Scm<sup>-1</sup> for H<sub>2</sub>SO<sub>4</sub>, 1175 ± 23 Scm<sup>-1</sup> for HNO<sub>3</sub> and 846 ± 72 Scm<sup>-1</sup> for HCl treatments followed by N<sub>2</sub> gas-passing with the pressure of 0.1 MPa. Corresponding power factor of 97 ± 8 μWm<sup>-1</sup>K<sup>-2</sup>, 121 ± 10 μWm<sup>-1</sup>K<sup>-2</sup> and 32 ± 1 μWm<sup>-1</sup>K<sup>-2</sup> were observed for H<sub>2</sub>SO<sub>4</sub>, HNO<sub>3</sub>, and HCl treatments, respectively. Based on our results, acids are mainly responsible for the removal of insulating PSS resulting in the conformational change of the PEDOT polymer chain while N<sub>2</sub> pressure is responsible for the additional conformation of PEDOT polymer favoring the linearly oriented structure. Therefore, mechanical force such as N<sub>2</sub> pressure after post-treatment of PEDOT:PSS with various acids can lead to additional conformation of the polymer and can result in higher thermoelectric performance.

## 2 Experimental details

PEDOT:PSS (Clevios PH 1000) was purchased from Heraeus Deutschland GmbH & Co. KG (Germany). Sulfuric acid (95%), nitric acid (69%) and hydrochloric acid (37%) from Wako Pure Chemical Industries Ltd. (Japan) were used as received in our experiment.

The glass substrates were washed with deionized (DI) water, ethanol, and acetone and finally cleaned in the Filgen UV ozone cleaner for 20 min. PEDOT:PSS film (100 μl) was prepared by spin-coating at a spin speed of 600 rpm for 30 s followed by 2000 rpm for 20 s.

**H<sub>2</sub>SO<sub>4</sub> treatment** PEDOT:PSS film was put on the hot plate at a temperature of 160 °C, then 100 μl of H<sub>2</sub>SO<sub>4</sub> was dropped onto it. After 10 min, N<sub>2</sub> gas was passed with a pressure of 0.1 MPa using gun. Then, the films were thoroughly rinsed with DI water and dried on the hot plate at a temperature of 120 °C for 15 min

**HNO<sub>3</sub> treatment** HNO<sub>3</sub> treatment was done as in our previous report [20]

**HCl treatment** HCl treatment was done the same procedure as the H<sub>2</sub>SO<sub>4</sub> treatment except the treatment temperature was at 70 °C

The films were fixed at 20 mm away from the gun for all experiments. All treatments were done at their optimized treatment temperatures and conditions. Figure 1 shows the process of N<sub>2</sub> gas-passing on the PEDOT:PSS films after treatment with various acids.

Electrical conductivity, Seebeck coefficient (thermo power) and power factor of the films were measured in a helium environment by ZEM-3M8 ULVAC (ADVANCED RIKO, Inc.), which is attached to the sample holder for the thin film measurement. Surface of the films was observed by digital microscope (OLYMPUS BX53M) at a magnification of 7.5×. Carrier concentration and carrier mobility were measured to examine the effect of N<sub>2</sub> on the improvement of electrical conductivity using Lake Shore Model 8403, AC/DC Hall effect measurement system. The change in bonding condition before and after treatment was analyzed by Raman spectroscopy (JASCO, NRS 450 NMDS) with a green laser (wavelength 532.21 nm). The morphology and surface roughness of the PEDOT:PSS films were observed by Scanning Probe Microscopy (SPM, Nano Navi SII). The removal of insulating PSS was confirmed by X-ray photoelectron spectroscopy (XPS, JEOL JPS 9030, Japan). UV–Vis-NIR (JASCO V-670 spectrophotometer) was performed to observe the doping states of the PEDOT. The change in crystallinity of PEDOT:PSS films after treatment at various pressures of N<sub>2</sub> gas was characterized by RIGAKU Smart-Lab X-ray diffractometer with CuK<sub>α</sub> radiation (λ = 1.5418° Å) at a scanning rate of 1 degree per minute.

## 3 Results and discussion

Electrical conductivity, Seebeck coefficient and power factor of pristine PEDOT:PSS are around 1.7 ± 0.2 Scm<sup>-1</sup>, 20 ± 1 μVK<sup>-1</sup> and 0.07 ± 0.005 μWm<sup>-1</sup>K<sup>-2</sup> at a measurement temperature of 423 K. Electrical conductivity

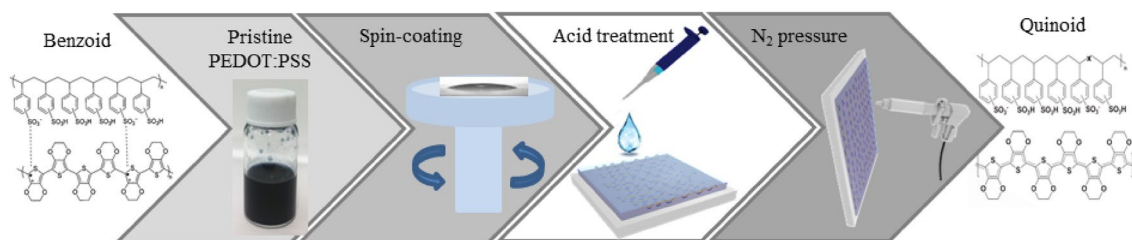


**Fig. 1** Schematic illustration of the experimental details

of  $\text{H}_2\text{SO}_4$ ,  $\text{HNO}_3$  and  $\text{HCl}$  treated PEDOT:PSS films are  $1400 \pm 210 \text{ Scm}^{-1}$ ,  $656 \pm 75 \text{ Scm}^{-1}$  and  $632 \pm 27 \text{ Scm}^{-1}$  respectively after washing with DI water. Electrical conductivity increased to  $1810 \pm 200 \text{ Scm}^{-1}$  for  $\text{H}_2\text{SO}_4$  treated,  $1175 \pm 23 \text{ Scm}^{-1}$  for  $\text{HNO}_3$  treated and  $846 \pm 72 \text{ Scm}^{-1}$  for  $\text{HCl}$  treated PEDOT:PSS films after  $\text{N}_2$  gas-passing with a pressure of 0.1 MPa as illustrated in Fig. 2a. All the measurements for electrical conductivity, Seebeck coefficient and power factor are carried out at 423 K in our experiments. The improvement in electrical conductivity after acids treatment followed by DI water-washing can be attributed to the removal of the insulating PSS, also resulting in the conformational change of the PEDOT polymer chain from benzoid (coiled) to quinoid (linear) structure [21–23]. In contrast, the improvement in the electrical conductivity after acids treatment followed by  $\text{N}_2$  gas-passing can be ascribed as the

additional conformational change of the PEDOT due to the pressure of  $\text{N}_2$  gas. It is confirmed by Raman spectroscopy as shown in Fig. 4. Seebeck coefficient does not change significantly for all acids except for  $\text{HNO}_3$  from  $27 \pm 1$  to  $32 \pm 1 \mu\text{VK}^{-1}$  (Fig. 2b) after DI water-washing and  $\text{N}_2$  gas-passing respectively, but which is still unclear why. The power factor improved from  $72 \pm 6$  to  $97 \pm 8 \mu\text{Wm}^{-1} \text{K}^{-2}$  for  $\text{H}_2\text{SO}_4$ , from  $46 \pm 3$  to  $121 \pm 10 \mu\text{Wm}^{-1} \text{K}^{-2}$  for  $\text{HNO}_3$  and  $26 \pm 1$  to  $32 \pm 1 \mu\text{Wm}^{-1} \text{K}^{-2}$  for  $\text{HCl}$  treated PEDOT:PSS films (Fig. 2c) after corresponding acid treatments followed by DI water-washing and  $\text{N}_2$  gas-passing at a pressure of 0.1 MPa. Therefore,  $\text{N}_2$  gas-passing after acid treatments can give the higher thermoelectric power factor values rather than DI water-washing after acid treatments. Electrical conductivity, Seebeck coefficient and power factor of  $\text{HNO}_3$  treated PEDOT:PSS films at different pressures of  $\text{N}_2$  gas are shown

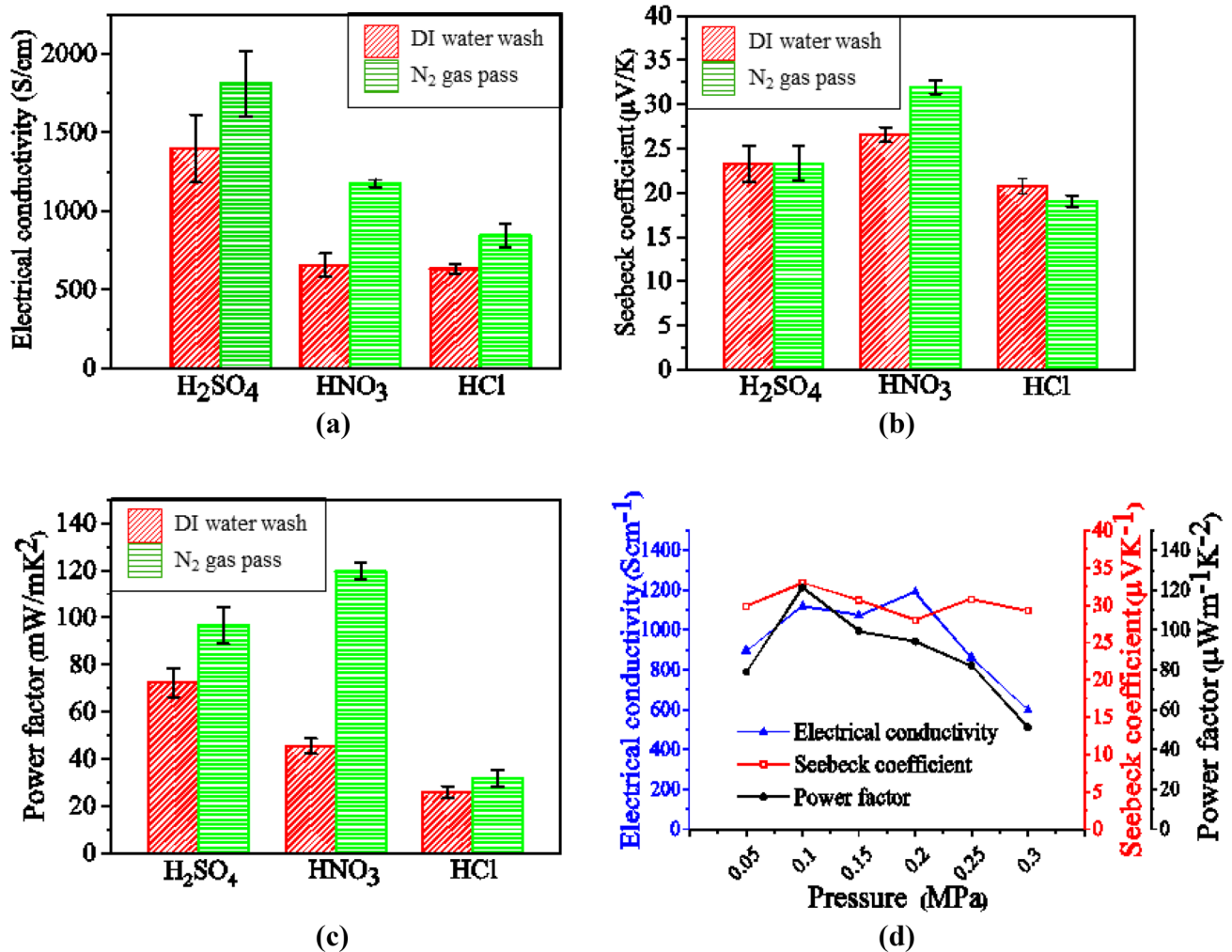


**Fig. 2** a Electrical conductivity, b Seebeck coefficient and c power factor of the PEDOT:PSS films treated with various acids followed by DI water-washing and passing with the pressure of  $\text{N}_2$  gas (0.1 MPa). d Electrical conductivity, Seebeck coefficient and power factor of the

$\text{HNO}_3$  treated PEDOT:PSS films followed by passing with different pressures of  $\text{N}_2$  gas such as 0.05 MPa, 0.1 MPa, 0.15 MPa, 0.2 MPa, 0.25 MPa and 0.3 MPa

in Fig. 2d. The electrical conductivity increases at the pressure range of 0.1 to 0.2 MPa and then decreases beyond 0.2 MPa. This is probably due to the film damage or some defects on the surface of the films because of the high pressure of  $N_2$  gas. These surface defects are observed by digital microscope as in Fig. 3. Smooth surface are observed in pristine PEDOT:PSS film and the film treated with a pressure of 0.1 MPa. Some pinholes or micropores are observed on the surface of the films treated at pressure of 0.15 and 0.2 MPa while big scratches are observed on the film treated with a pressure of 0.25 MPa.

The optimum Seebeck coefficient of  $32 \pm 1 \mu\text{VK}^{-1}$  was obtained at a pressure of 0.1 MPa. Seebeck coefficient is defined by

$$S = \frac{\pi^2 k_B^2 T}{3e} \left. \frac{\partial \ln \sigma(E)}{\partial E} \right|_{E_f} \quad (1)$$

where  $\sigma(E)$  is the conductivity of the material at Fermi energy  $E_f$ ,  $k_B$  is the Boltzmann constant and  $e$  is the charge of the electron [24, 25]. Based on this equation, Seebeck coefficient also depends on the local band structure of the material. The removal of PSS may transform the local band structure of PEDOT:PSS and such a probable change in the band structure may be responsible for the improvement in the Seebeck coefficient [26]. Unfortunately, we failed to do experiment at a pressure of 0.1 MPa in our previous report [20]. Nevertheless, the optimum power factor of  $121 \pm 10 \mu\text{Wm}^{-1}\text{K}^{-2}$  was obtained by the treatment with  $\text{HNO}_3$  at a pressure of 0.1 MPa due to the high Seebeck coefficient.

We observed that the pressure of  $N_2$  gas favors the phase segregation of PSS as well as the conformation of the PEDOT polymer chain resulting in the enhancement of the carrier concentration, especially the carrier mobility. It is confirmed by the Hall measurement as shown in Table (1). Pristine PEDOT:PSS film has hole mobility of around  $2.4 \pm 0.3 \text{ cm}^2\text{V}^{-1}\text{s}^{-1}$  and hole concentration of an order of  $17 \text{ cm}^{-3}$ . After treatment with  $\text{HNO}_3$  and passing with  $N_2$  gas

**Table 1** Carrier mobility and carrier concentration of the pristine PEDOT:PSS and those of  $\text{HNO}_3$  treated films at various pressures of  $N_2$  gas

Sample	$\mu$ ( $\text{cm}^2\text{V}^{-1}\text{s}^{-1}$ )	$n$ ( $\text{cm}^{-3}$ )
Pristine	$2.4 \pm 0.3$	$(7.4 \pm 1.7) \times 10^{17}$
0.05 MPa	$5.1 \pm 0.7$	$(4.4 \pm 0.02) \times 10^{21}$
0.1 MPa	$6.9 \pm 1.4$	$(2.1 \pm 0.5) \times 10^{21}$
0.15 MPa	$4.9 \pm 0.2$	$(3.4 \pm 0.3) \times 10^{21}$
0.2 MPa	$5.6 \pm 1.3$	$(2.7 \pm 0.6) \times 10^{21}$
0.25 MPa	$5.1 \pm 0.7$	$(5.1 \pm 0.6) \times 10^{21}$
0.3 MPa	8	$3.3 \times 10^{21}$

at various pressures, the hole concentration enhanced to an order of  $21$  and the hole mobilities are also improved. The optimum carrier mobility of  $7 \pm 1.4 \text{ cm}^2\text{V}^{-1}\text{s}^{-1}$  is obtained for the sample treated at a pressure of 0.1 MPa while the carrier concentrations are not too much different at various pressures of  $N_2$  gas. Therefore, the pressure of the  $N_2$  gas can lead to the linear orientation of the polymer structure. The carrier mobility decreases again beyond the pressure of 0.1 MPa and this may be attributed to the defects on the surface of the films such as pin holes and damages, which is also consistent with the digital micrographs.

Raman spectroscopy was also performed to confirm the effect of the pressure of  $N_2$  gas on the conformation of the PEDOT polymer chain. Calibration was performed using Si substrate before and after sample measurement in order to investigate the potential heating effect on the spectrum. No significant peak shift was found for the calibration results, indicating that there was no potential heating effect on the spectral peak position. The peaks assigned at  $1227 \text{ cm}^{-1}$  in Fig. 4 come from  $C_\alpha-C_\alpha$  inter-ring stretching,  $1337 \text{ cm}^{-1}$  from  $C_\beta-C_\beta$  inter-ring stretching,  $1401 \text{ cm}^{-1}$  from  $C_\alpha=C_\beta$  symmetric stretching,  $1506 \text{ cm}^{-1}$  from  $C_\alpha=C_\beta$  asymmetric stretching, respectively [21–23, 27, 28]. The peak at  $1401 \text{ cm}^{-1}$  shifts to  $1404 \text{ cm}^{-1}$ ,  $1406 \text{ cm}^{-1}$ ,  $1407 \text{ cm}^{-1}$ ,  $1408 \text{ cm}^{-1}$  and  $1409 \text{ cm}^{-1}$ , respectively after treatment with

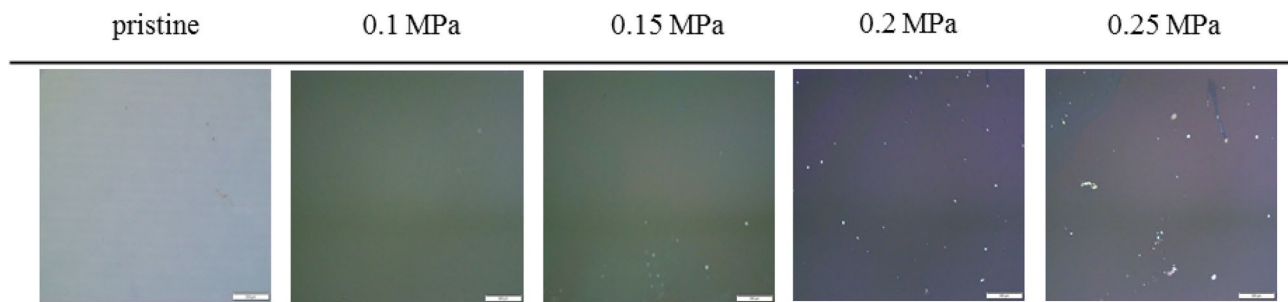


**Fig. 3** Digital micrographs of  $\text{HNO}_3$  treated PEDOT:PSS films showing the surface condition at various pressures of  $N_2$  gas. The scale bars in all photos are  $500 \mu\text{m}$ . All photos were captured at a magnification of  $7.5\times$

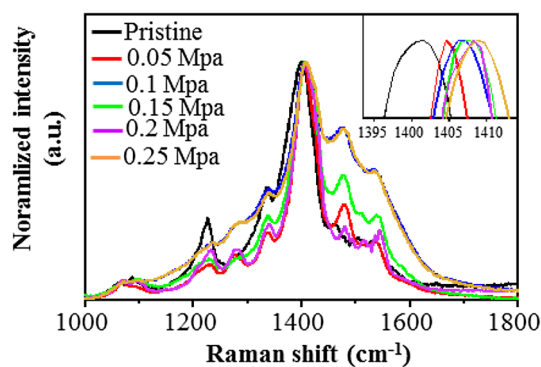


**Fig. 4** Raman spectra of pristine and  $\text{HNO}_3$  treated PEDOT:PSS films at different pressures of  $\text{N}_2$  gas. The inset illustrates the zoom-in view of the peaks shift of  $\text{C}\alpha=\text{C}\beta$  symmetric stretching

$\text{HNO}_3$  and the pressure of  $\text{N}_2$  gas at 0.05 MPa, 0.1 MPa, 0.15 MPa, 0.2 MPa and 0.25 MPa respectively. These peaks shift reveal the conformation of the PEDOT from benzoid (coiled) to quinoid (linear) structure [21–23]. Therefore, the pressure of the  $\text{N}_2$  gas after acid treatment can favor the linearly oriented structure of the PEDOT, resulting in the enhancement of the electrical conductivity which is also consistent with the Hall measurement. It was observed in the previous reports that oriented mechanical forces induced by directional film deposition methods [29, 30], mechanical rubbing [31] and capillary force [32] makes the polymer films highly aligned and causes anisotropic charge transport in the film. Similar to prior reports,  $\text{N}_2$  blown from one side of the sample might include oriented mechanical force, creating the anisotropic alignment in the PEDOT:PSS and leading to increase in electrical conductivity.

In order to observe the morphological changes of PEDOT:PSS at various pressures of  $\text{N}_2$  gas, the SPM images were scanned for the pristine PEDOT:PSS films and the  $\text{HNO}_3$  treated films. Figure 5 represents the topography and phase images of the pristine and  $\text{HNO}_3$ -treated PEDOT:PSS films at various pressures of  $\text{N}_2$  gas at 0.05 MPa, 0.1 MPa, 0.15 MPa, 0.2 MPa and 0.25 MPa respectively. The bright region represents the PEDOT and the dark brown region represents the PSS in the phase images of the films. We can see clearly that some dark colored regions disappear after the treatment in the phase images. It can be attributed to the partial removal of PSS ions [33]. In the topographic images, the root mean square (rms) roughness of the pristine PEDOT:PSS film is 1.2 nm. However, the rms roughness of the treated films become 1.3 nm, 1.5 nm, 1.4 nm, 1.7 nm and 2.0 nm at the  $\text{N}_2$  pressures of 0.05 MPa, 0.1 MPa, 0.15 MPa, 0.2 MPa and 0.25 MPa respectively. It is an evidence of the phase separation of PSS from PEDOT indicating the removal of PSS phase [34]. Interestingly, the rms of the pristine and the  $\text{HNO}_3$  treated samples at  $\text{N}_2$  pressures of 0.05 MPa, 0.1 MPa and 0.15 MPa are not too much different,

nevertheless, those of the treated samples at 0.2 MPa and 0.25 MPa significantly increase to 1.7 nm and 2.0 nm. Therefore, the pressure of  $\text{N}_2$  gas favors the smoother surface morphology even though there is phase separation between the PEDOT and PSS grains. On the other hand, the higher pressure of  $\text{N}_2$  gas leads to the surface defects like pin holes, resulting in the increase of rms values.

XPS was conducted to analyze the influence of the pressure of  $\text{N}_2$  gas on the removal of extra PSS phase of the  $\text{HNO}_3$  treated PEDOT:PSS films. XPS bands at 169.1 eV and 167.7 eV are the S2p bands of the sulfur atoms in PSS and the bands at 164.3 eV and 163.1 eV are the S2p bands of the sulfur atoms in PEDOT [35] as in Fig. 6a. The S2p peaks of PSS shifts around 1 eV to the lower binding energy after the treatment with  $\text{HNO}_3$  followed by passing at various pressures of  $\text{N}_2$  gas. The atomic ratio of PEDOT:PSS was calculated from the area under the peaks using full width at half maximum (FWHM) of curve fitting. The ratio of PEDOT to PSS before treatment is 1:2.52. These ratios significantly increase to 1:0.41, 1:0.44, 1:0.58, 1:0.59 and 1:0.4 after treatment with  $\text{HNO}_3$  followed by the pressure of  $\text{N}_2$  gas at 0.05 MPa, 0.1 MPa, 0.15 MPa, 0.2 MPa and 0.25 MPa respectively. Nevertheless, the ratios are not significantly different at different pressures of  $\text{N}_2$  gas. Therefore,  $\text{HNO}_3$  treatment is essentially responsible for the removal of insulating PSS and, on the other words, the pressure of  $\text{N}_2$  gas after  $\text{HNO}_3$  treatment does not play a major role in removing the extra PSS. The peaks at 285.7 eV and 284 eV in C1 s spectra come from the C–O bond in PEDOT and C–C bond in PSS chain (Fig. 6b) [36]. After treatment with  $\text{HNO}_3$  and passing with various pressures of  $\text{N}_2$  gas, the intensities of the peaks at 285.7 eV increase while the intensities of the peaks at 284 eV decrease, indicating the removal of thiophene group of PSS. The peaks at 531.4 eV and 532.5 eV in Fig. 6c come from the oxygen atom which is attached to the sulfur atom in PSS and the oxygen atom in PEDOT. After treatment, the intensities of the peaks at higher binding energy increases while the intensities of the peaks at lower binding energy decreases. It can be attributed to the phase segregation of PSS from the PEDOT:PSS resulting in the formation of PSSH [34, 35]. However, by comparing the XPS results of the treated films at different pressures of  $\text{N}_2$  gas, the intensities of the peaks are very similar to each other. It means that passing with  $\text{N}_2$  gas after acid treatment does not play a major role in the removal of PSS.

UV–vis–NIR absorption spectra were recorded to confirm the above XPS analysis as illustrated in Fig. 7a and b. The decrease in the intensities of the two absorption bands at 196 nm and 225.8 nm in the UV region (Fig. 7a) after acid treatment followed by passing with  $\text{N}_2$  gas at various pressures indicates the removal of extra PSS from PEDOT:PSS, hence both bands come from the PSS moiety [36]. However, all the bands stack one upon another after

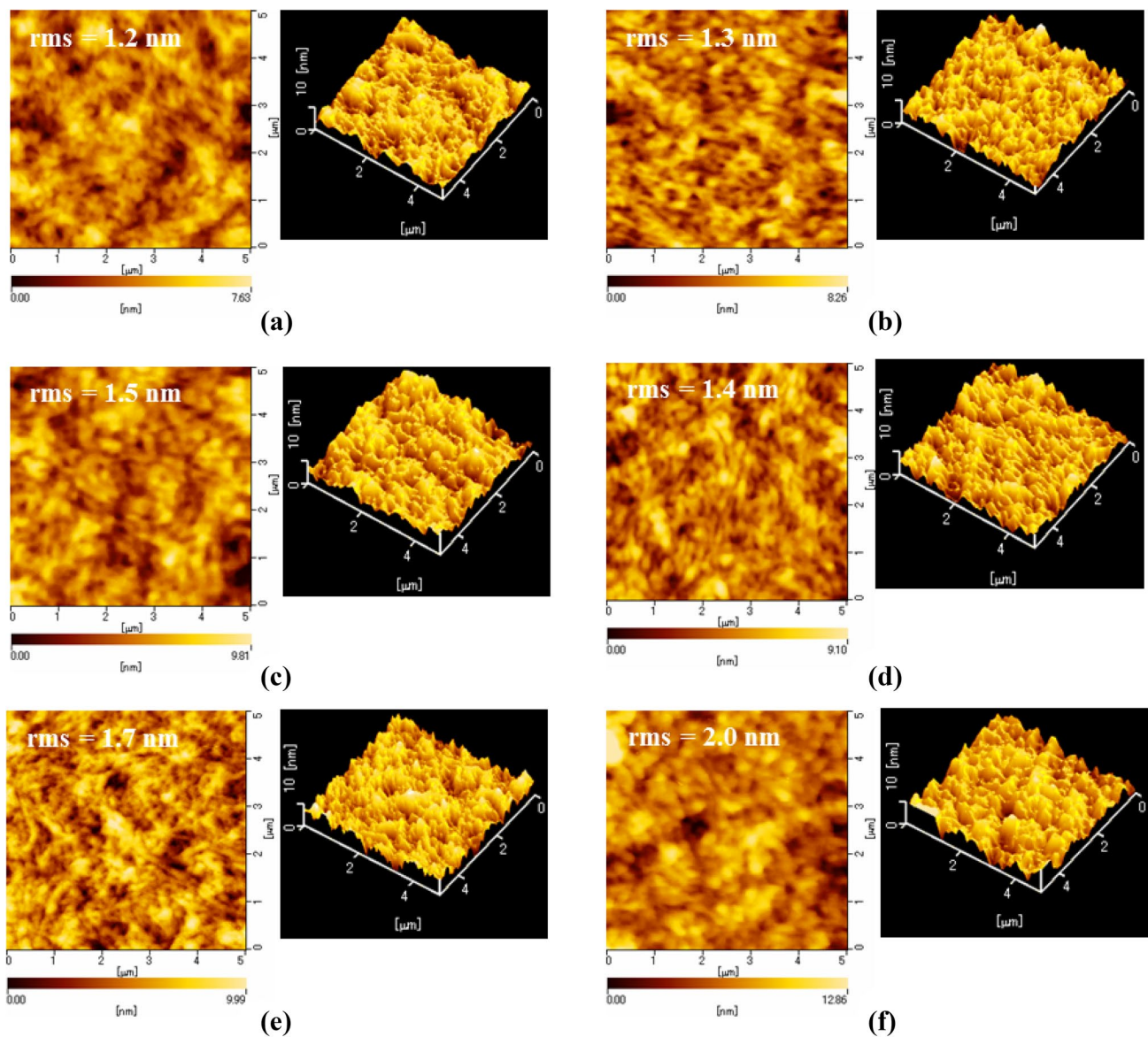


**Fig. 5** SPM topography images and phase images of **a** pristine PEDOT:PSS films and those of  $\text{HNO}_3$  treated films at  $\text{N}_2$  gas pressure of **b** 0.05 MPa, **c** 0.1 MPa, **d** 0.15 MPa, **e** 0.2 MPa and **f** 0.25 MPa. The scanned area for each image is  $5 \mu\text{m} \times 5 \mu\text{m}$

$\text{HNO}_3$  treatment at various pressures of  $\text{N}_2$  gas show that the amount of PSS removal is similar at different treatment pressures. The absorption bands at near infrared region were also recorded to examine the influence of  $\text{N}_2$  pressure after treatment. The absorption bands around 600 nm, 900 nm and 1200 nm come from the neutral, polaron and bipolaron states of the PEDOT, which have reported in the previous literature [36]. The improvement of the absorption intensities at  $\approx 900$  nm after  $\text{HNO}_3$  treatment and at various pressures of  $\text{N}_2$  gas reveals an increase in its doping state to polaronic state. Therefore, the results of UV-vis-NIR measurement agree well with XPS measurement.

To investigate the mechanism of significantly increasing the electrical conductivity after acid treatment followed by  $\text{N}_2$  gas-passing, X-ray diffraction (XRD) was performed as depicted in Fig. 8. The pristine PEDOT:PSS film shows only the amorphous halo inter-chain stacking at  $2\theta$  value of  $23.8^\circ$ . After treatment with  $\text{HNO}_3$  and at various pressures of  $\text{N}_2$  gas, the new peaks appear at around  $2.5^\circ$  and  $6.8^\circ$ , which are attributed to the lamellae stacking of the alternating structure of PEDOT and PSS. Therefore, after acid treatment, PEDOT crystallites incline to a linear structure resulting in more lamellae stacking [37–39], which is consistent with the Raman spectroscopy results. Moreover, no significant peaks shifts are observed for the positions of both peaks resulting

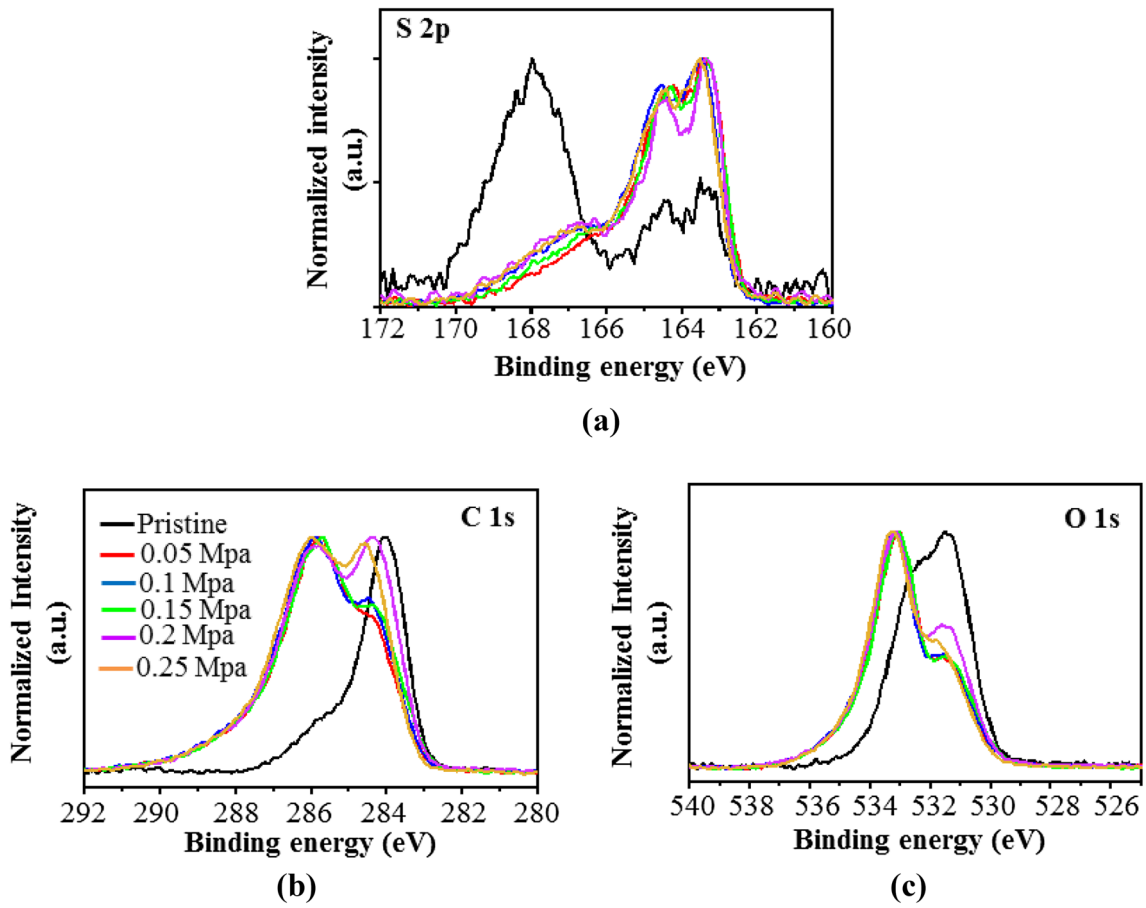


**Fig. 6** a The S2p, b C1s and c O1s core-level of the XPS spectra of the pristine and those of HNO<sub>3</sub> treated PEDOT:PSS films at different N<sub>2</sub> pressures

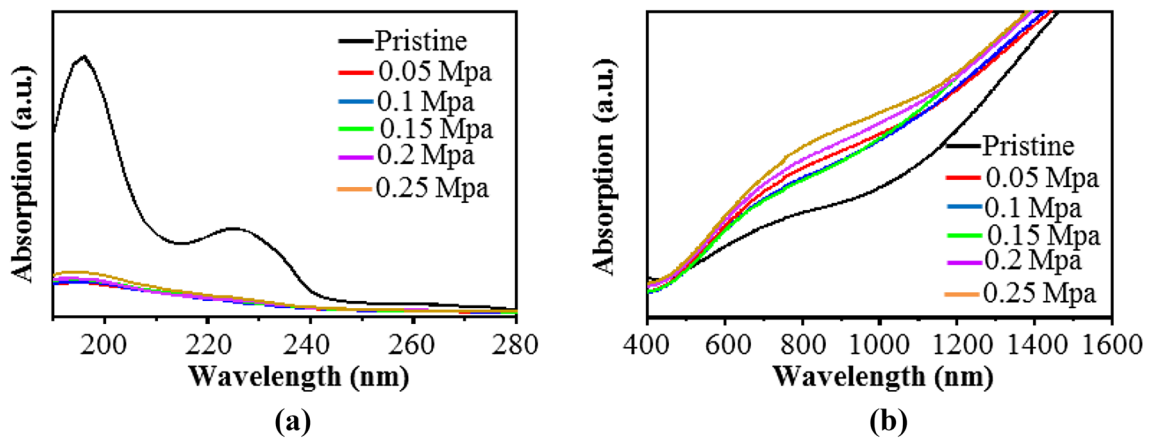


**Fig. 7** UV-Vis-NIR spectra of pristine and HNO<sub>3</sub> treated PEDOT:PSS at different pressures of N<sub>2</sub> gas: a at UV region and b at vis-NIR region

in no obvious changes of lattice spacing although different pressures of N<sub>2</sub> gas are used. Therefore, it can be ascribed

as the pressure of N<sub>2</sub> gas has no significant influences on the removal of extra PSS.

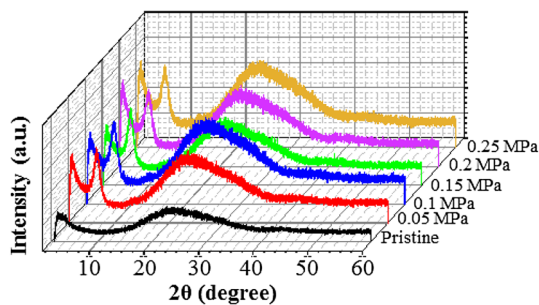


**Fig. 8** X-ray diffraction (XRD) pattern of pristine and those of  $\text{HNO}_3$  treated PEDOT:PSS thin films followed by passing with different pressures of  $\text{N}_2$  gas

## 4 Conclusion

In summary, we have reported the influence of the pressure of  $\text{N}_2$  gas after acid treatment on the structure and thermoelectric properties of PEDOT:PSS. The improvement of electrical conductivity is due to the removal of insulating extra PSS from PEDOT:PSS and the conformation of PEDOT polymer structure from benzoid (coiled) to quinoid (linear) structure. In our experiment, there are two reasons for the conformation of PEDOT: (1) the removal of PSS by acid treatments and (2) the pressure of  $\text{N}_2$  gas. Acid treatment plays a major role in the removal of the insulating PSS, resulting in the conformation of PEDOT while the pressure of  $\text{N}_2$  gas is mainly responsible for the additional conformation of polymer favoring the linear orientation of the structure. Therefore, mechanical forces such as the pressure of  $\text{N}_2$  gas can affect the structure of acid-treated PEDOT: PSS regardless of the types of acids. Applying mechanical forces after acid treatment can give higher thermoelectric performance rather than traditional DI water-washing for PEDOT:PSS films.

**Acknowledgements** This work was partially supported by the JSPS KAKENHI (Grant Numbers 17K20065 and 18H01708). AKKK would like to thank financial support from Shenzhen Science, Technology and Innovation Commission (Basic Research Project (No. JCYJ20180305180645221) and Shenzhen Peacock Team Project (No. KQTD2016030111203005)).

## Compliance with ethical standards

**Conflict of interest** The authors declare that there are no conflicts of interest.

## References

- R. Toshima, Recent progress of organic and hybrid thermoelectric materials. *Synth. Metal* **225**, 3–21 (2017)
- K. Prashantha, S. Wango, Smart power generation from waste heat by thermoelectric generator. *Int. J. Mech. Prod. Eng., Special Issue* (2016)
- M. Culebras, A.M. Igual-Muñoz, C. Rodriguez-Fernández, M.I. Gómez-Gómez, C. Gómez, A. Cantarero, Manufacturing Te/PEDOT films for thermoelectric application. *ACS Appl. Mater. Interfaces* **9**(24), 20826–20832 (2017)
- E. Jang, A. Poosapati, D. Madan, Enhanced thermoelectric properties of F4TCNQ doped P3HT and its use as a binder for  $\text{Sb}_2\text{Te}_3$  based printed thermoelectric films. *ACS Appl. Energy Mater.* **1**(4), 1455–1462 (2018)
- G. Chen, W. Xu, D. Zhu, Recent advances in organic polymer thermoelectric composites. *J. Mater. Chem. C* **5**, 4350–4360 (2017)
- M. Culebras, C. Cho, M. Kreckler, R. Smith, Y. Song, M. Clara, C.M. Gomez, A. Cantarero, J.C. Grunlan, High thermoelectric power factor organic thin films through combination of nanotube multilayer assembly and electrochemical polymerization. *ACS Appl. Mater. Interfaces* **9**(7), 6306–6313 (2017)
- J. Li, Y. Du, R. Jia, J. Xu, S.Z. Shen, Thermoelectric properties of flexible PEDOT:PSS/polypyrrole/paper nanocomposite films. *Mater. (Basel)* **10**(7), 780 (2017)
- Z. Zhu, C. Liu, F. Jiang, J. Xu, E. Liu, Effective treatment methods on PEDOT:PSS to enhance its thermoelectric performance. *Synth. Metals* **225**, 31–40 (2017)
- J. Luo, D. Billep, T. Waechter, T. Otto, M. Toader, O. Gordan, E. Sheremet, J. Martin, M. Hietschold, D.R.T. Zahn, T. Gessner, Enhancement of the thermoelectric properties of PEDOT:PSS thin films by post-treatment. *J. Mater. Chem. A* **1**, 7576–7583 (2013)
- J.S. Kim, W. Jang, D. Wand, The investigation of the seebeck effect of the poly (3,4-Ethylenedioxythiophene)-tosylate with the various concentrations of an oxidant. *Polymers* **11**(1), 21 (2019)
- V. Andrei, K. Bethke, F. Madzharova, S. Beeg, A. Knop-Gericke, J. Kneipp, K. Rademann, Size dependence of electrical conductivity and thermoelectric enhancements in spin-coated PEDOT:PSS single and multiple layers. *Adv. Electron. Mater.* **3**, 2 (2017)
- N. Dubey, M. Leclerc, Conducting polymers: efficient thermoelectric materials. *J. Polym. Sci.* **49**(7), 467–475 (2011)
- Q. Meng, Q. Jiang, K. Cai, L. Chen, Preparation and thermoelectric properties of PEDOT:PSS coated Te nanoroad/PEDOT:PSS composite films. *Org. Electron.* **64**, 79–85 (2019)
- H. Shi, C. Liu, Q. Jiang, J. Xu, Effective approach to improve the electrical conductivity of PEDOT:PSS: a review. *Adv. Electron. Mater.* **1**, 4 (2015)
- S.H. Lee, H. Park, W. Son, H.H. Choi, J.H. Kim, Novel solution-processable dedoped semiconductors for application in thermoelectric devices. *J. Mater. Chem. A* **2**, 13380–13387 (2014)
- X. Wang, A.K.K. Kyaw, C. Yin, F. Wang, Q. Zhu, T. Tang, P.I. Yee, J. Xu, Enhancement of thermoelectric performance of PEDOT:PSS films by post-treatment with a superacid. *RSC Adv* **8**, 18334–18340 (2018)
- Z. Fan, P. Li, D. Du, J. Ouyang, Significantly enhanced thermoelectric properties of PEDOT:PSS films through sequential post-treatments with common acids and bases. *Adv. Energy Mater.* **7**, 8 (2017)
- W. Meng, R. Ge, Z. Li, J. Tong, T. Liu, Q. Zhao, S. Xiong, F. Jiang, L. Mao, Y. Zhou, Conductivity enhancement of PEDOT:PSS films via phosphoric acid treatment for flexible all-plastic solar cells. *ACS Appl. Mater. Interfaces.* **7**(25), 14089–14094 (2015)
- A.K.K. Kyaw, T.A. Yemata, X. Wang, S.L. Lim, W.S. Chin, K. Hippalgaonkar, J. Xu, Enhanced thermoelectric properties of PEDOT:PSS films by sequential post-treatment with formamide. *Macromol. Mater. Eng.* **303**, 1700429 (2018)
- M.T. Myint, M. Hada, H. Inoue, T. Marui, T. Nishikawa, M. Umeno, S. Ichimura, Y. Nishina, A.K. Kyaw, Y. Hayashi, Simultaneous improvement in electrical conductivity and seebeck



- coefficient of PEDOT:PSS by N<sub>2</sub> pressure-induced nitric acid treatment. *RSC Adv.* **8**, 36563 (2018)
21. S.R.S. Kumar, N. Kurra, H.N. Alshareef, Enhanced high temperature thermoelectric response of sulfuric acid treated conducting polymer thin films. *J. Mater. Chem. C* **4**, 215–221 (2016)
  22. Y. Xia, J. Ouyang, Significant conductivity enhancement of conductive poly (3,4-ethylenedioxythiophene): poly (styrenesulfonate) films through a treatment with organic carboxylic acids and inorganic acids. *ACS Appl. Mater. Interfaces* **2**(2), 474–483 (2010)
  23. Z. Zhu, C. Liu, H. Shi, Q. Jiang, J. Xu, F. Jiang, J. Xiong, E. Liu, An effective approach to enhance thermoelectric properties of PEDOT:PSS films by a DES post-treatment. *J. Polym. Sci. Part B* **53**(12), 885–892 (2015)
  24. J. Kim, J.G. Jang, J.-I. Hong, S.H. Kim, J. Kwak, Sulfuric acid vapour treatment for enhancing the thermoelectric properties of PEDOT:PSS thin-film. *J. Mater. Sci.* **27**, 6122–6127 (2016)
  25. Y. Zheng, Y. Luo, C. Du, B. Zhu, Q. Liang, H.H. Hng, K. Hip-palgaonkar, J. Xu, Q. Yan, Designing hybrid architectures for advanced thermoelectric materials. *Mater. Chem. Front.* **1**, 2457–2473 (2017)
  26. A. Mazaheripour, S. Majumdar, D. Hanemann-Rawlings, E.M. Thomas, C. MacGuinness, L. d'Alencon, M.L. Chabinyk, R.A. Segalman, Tailoring the seebeck coefficient of PEDOT:PSS by controlling ion stiochoimetry in ionic liquid additives. *Chem. Mater.* **30**, 4816–4822 (2018)
  27. J. Wang, K. Cai, S. Shen, Enhanced thermoelectric properties of poly (3,4-ethylenedioxythiophene) thin films treated with H<sub>2</sub>SO<sub>4</sub>. *Org. Electron.* **15**(11), 3087–3095 (2014)
  28. M.S. Mahajan, D.M. Marathe, S.S. Ghosh, V. Ganesan, J.V. Sali, Changes in in-plane electrical conductivity of PEDOT:PSS thin films due to electric field induced dipolar reorientation. *RSC Adv.* **5**, 86393–86401 (2015)
  29. L. Li, P. Gao, K.C. Schuermann, S. Ostendorp, W. Wang, C. Du, Y. Lei, H. Fuchs, L.D. Cola, K. Müllen, L. Chi, Controllable growth and field-effect property of monolayer to multilayer micro-strips of an organic semiconductor. *J. Am. Chem. Soc.* **132**(26), 8807–8809 (2010)
  30. A.K.K. Kyaw, L.S. Lay, G.W. Peng, J. Changyun, Z. Jie, A nanogroove-guided slot-die coating technique for highly ordered polymer films and high-mobility transistors. *Chem. Commun.* **52**, 358–361 (2016)
  31. C.Y. Yang, C. Soci, D. Moses, A.J. Heeger, Aligned rrP3HT film: structural order and transport properties. *Synth. Met.* **155**, 639–642 (2005)
  32. C. Luo, A.K.K. Kyaw, L.A. Perez, S. Patel, M. Wang, B. Grimm, G.C. Bazan, E.J. Kramer, A.J. Heeger, General strategy for self-assembly of highly oriented nanocrystalline semiconducting polymers with high mobility. *Nano Lett.* **14**(5), 2764–2771 (2014)
  33. T.-C. Tsai, H.-C. Chang, C.-H. Chen, Y.-C. Huang, W.-T. Whang, A facile dedoping approach for effectively tuning thermoelectricity and acidity of PEDOT:PSS films. *Org. Electron.* **15**, 641–645 (2014)
  34. C. Yeon, S.J. Yun, J. Kim, J.W. Lim, PEDOT:PSS films with greatly enhanced conductivity via nitric acid treatment at room temperature and their application as Pt/TCO-free counter electrodes in dye-sensitized solar cells. *Adv. Electron. Mater.* **1**, 1500121 (2015)
  35. S.H. Chang, C.H. Chiang, F.S. Kao, C.L. Tien, C.G. Wu, Unraveling the enhanced electrical conductivity of PEDOT:PSS thin films for ITO-free organic photovoltaics. *IEEE Photon.* **6**(4), 8400 (2014)
  36. D.A. Mengistie, M.A. Ibrahim, P.C. Wang, C.W. Chu, Highly conductive PEDOT:PSS treated with fomic acid for ITO-free polymer solar cell. *ACS Appl. Mater. Interfaces* **6**(4), 2292–2299 (2014)
  37. H. Park, S.H. Lee, F.S. Kim, H.H. Choi, I.W. Cheong, J.H. Kim, Enhanced thermoelectric properties of PEDOT:PSS nanofilms by a chemical dedoping process. *J. Mater. Chem. A* **2**, 6532 (2014)
  38. A.K. Sarker, J. Kim, B.-H. Wee, H.-J. Song, Y. Lee, J.-D. Hong, C. Lee, Hydroiodic acid treated PEDOT:PSS thin films as transparent electrodes: an approach towards ITO free organic photovoltaics. *RSC Adv.* **5**, 52019 (2015)
  39. A. Hu, L. Tan, X. Hu, L. Hu, Q. Ai, X. Meng, L. Chen, Y. Chen, Crystallization and conformation engineering of solution-processed polymer transparent electrodes with high conductivity. *J. Mater. Chem. C* **5**, 382 (2017)

**Publisher's Note** Springer Nature remains neutral with regard to jurisdictional claims in published maps and institutional affiliations.